

Supporting Information

Facile Modification of Multi-resonance Acceptors and Donors in Intramolecular TSCT-TADF Emitters for OLEDs: A Computational Study

Singaravel Nathiya,¹ Murugesan Panneerselvam*^{1,2} and Luciano T Costa*¹

¹MolMod-CS - Instituto de Química, Universidade Federal Fluminense, Campos Valonginho s/n, Centro, Niterói 24020-14, Rio de Janeiro, Brazil.

²Programa de Engenharia Química (PEQ/COPPE), Universidade Federal do Rio de Janeiro (UFRJ), Moniz Aragão, Rio de Janeiro, 21941-594, RJ, Brazil.

*Corresponding Authors: E-mail: panneerchem130491@gmail.com & lucosta@id.uff.br

CONTENT CAPTIONS

Tables/Figures		Pages
Table S1	Calculated the HOMO energy of the reference molecules using various functionals at 6-31+G(d) basis set. (All energies are in eV)	S2
Table S2	Calculated the vertical singlet (S ₁) and triplet (T ₁) energies, singlet-triplet energy differences (ΔE_{ST}), and absorption wavelength (λ_{abs}) of reference molecules at 6-31+G(d) basis set along with experimental values. (All energies are in eV)	S2
Table S3	Calculated bond angles (°) and dihedral angles (°) for designed molecules at optimized S ₀ state at B3LYP/6-31+G(d) level of theory.	S2
Table S4	Calculated the emission (λ_{emi}) wavelength (in nm), overlap extent (λ_{OC} in %) for vertical singlet (S ₁) and triplet (T ₁) energies, and oscillator strength (f_{emi}) at PBE0/6-31+G(d) level of theory.	S3
Table S5	Charge transfer analysis based on the S ₁ state through interfragment charge transfer (IFCT) among the designed molecular fragments.	S5
Table S6	Calculated the intramolecular reorganization energies for selected molecules at PBE1PBE/6-31+G(d) level of theory.	S6
Table S7	Calculated the delayed fluorescence rate (K_{TADF} in 10 ⁺⁰⁵ s ⁻¹), internal quantum efficiency (Φ_{IQE}), external quantum efficiency (Φ_{EQE} %), photoluminescence quantum yield (PLQY %), and (FWHM nm) for three molecules.	S7
Table S8	Calculated the Huang-Rhys factors for molecule 1.	S7
Figure S1	Structural comparison between the crystal structure (violet) and the optimized S ₁ state (red) of molecule (1), calculated using various functionals with the 6-31+G(d) basis set.	S8
Figure S2	Comparison of HOMO energy for experimental molecules with computed results at different functionals with 6-31+G(d) basis set.	S9
Figure S3	Comparison of absorption wavelength (λ_{abs}) for experimental molecules with computed results at different functionals with 6-31+G(d) basis set.	S9
Figure S4	Optimized geometry of designed molecules (1-9) at B3LYP/6-31+G(d) level of theory.	S10
Figure S5	Optimized geometry of designed molecules (10-18) at B3LYP/6-31+G(d) level of theory.	S11

Figure S6	The selected bond length (l), dihedral angles (δ), and bond angle (θ) for designed molecules	S12
Figure S7	Structural differences between the S_1 and T_1 states for designed molecules (color codes: blue for S_1 and red for T_1).	S12
Figure S8	Structural differences between the S_0 and S_1 states for designed molecules (color codes: green for S_0 and blue for S_1).	S13
Figure S9	Visualization of non-covalent interactions (NCI) through RDG isosurfaces and scatter plots for (10-18) molecules.	S13
Figure S10	Frontier molecular orbital (FMOs) and optimized geometries of core donors (iso-surface value = 0.02 au) using B3LYP/6-31+G(d) level of theory.	S14
Figure S11	Frontier molecular orbital (FMOs) and optimized geometries of core acceptors (iso-surface value = 0.02 au) using B3LYP/6-31+G(d) level of theory.	S14
Figure S12	NTOs (iso-surface value = 0.02 a.u.) of designed molecules for T_1 state at PBE0/6-31+G(d) in the toluene medium.	S15
Figure S13	NTOs (iso-surface value = 0.02 a.u.) of designed molecules for T_2 state at PBE0/6-31+G(d) in the toluene medium.	S16
Figure S14	NTOs (iso-surface value = 0.02 a.u.) of designed molecules for T_3 state at PBE0/6-31+G(d) in the toluene medium.	S17
Figure S15	Spin density distributions of the designed molecules in their T_1 state, computed at the PBE0/6-31+G(d) level of theory.	S18
Figure S16	The effective rate RISC rate (K_{RISC}^{eff}) constant for all designed molecules.	S18
Figure S17	Calculated HR factors of all vibrational modes and reorganization energy (in red colour) in the $S_1 \rightarrow S_0$ transition of molecules 1, 4, 5, & 6.	S19

Table S1. Calculated the HOMO energies of the reference molecules using various functionals at 6-31+G(d) basis set. (All energies are in eV)

Molecules	B3LYP	PBE0	M06	M06-2X	CAM-B3LYP	WB97XD	Exp. ¹
HOMO							
1	-5.52	-5.68	-5.77	-6.64	-6.77	-7.30	-5.48
10	-5.56	-5.73	-5.82	-6.67	-6.81	-7.30	-5.53

Table S2. Calculated the vertical singlet (S₁) and triplet (T₁) energies, singlet-triplet energy differences (ΔE_{ST}), and absorption wavelength (λ_{abs} in nm) of reference molecules at 6-31+G(d) basis set along with experimental values. (All energies are in eV)

Molecules	B3LYP	PBE0	M06	M06-2X	CAM-B3LYP	WB97XD	Exp. ¹
S₁							
1	3.07	3.26	3.34	3.81	3.82	3.88	-
10	3.11	3.29	3.38	3.82	3.83	3.88	-
T₁							
1	2.85	2.90	2.88	3.24	2.91	3.07	-
10	2.86	2.91	2.89	3.25	2.92	3.08	-
ΔE_{ST}							
1	0.21	0.36	0.46	0.57	0.92	0.81	0.28
10	0.25	0.39	0.49	0.57	0.91	0.80	0.31
λ_{abs}							
1	404	380	370	325	324	319	378
10	399	376	366	324	323	319	380

Table S3. Calculated bond angles (°) and dihedral angles (°) for designed molecules at optimized S₀ state at B3LYP/6-31+G(d) level of theory.

Molecules	δ_1	δ_2	δ_3	δ_4	θ_1	θ_2
1	-120.63	55.45	-105.52	71.44	131.12	122.38
2	-119.88	56.35	-106.48	70.65	131.21	104.91
3	-119.44	57.23	-107.85	69.48	131.14	99.46
4	-120.66	55.54	-103.37	73.31	131.22	122.42
5	-126.21	57.94	-106.86	70.05	131.32	104.88
6	-131.85	53.33	-102.66	74.04	131.39	100.06
7	-132.42	53.00	-108.77	67.13	131.20	122.41
8	-128.78	56.22	-111.83	64.16	131.56	104.98
9	-127.55	57.34	-112.65	63.43	131.55	99.70
10	-125.64	57.95	-104.58	71.96	131.03	122.41
11	-125.36	58.06	-103.71	72.99	131.07	104.91
12	-118.22	58.86	-104.17	72.67	130.96	99.52
13	-116.58	59.54	-100.97	75.54	131.07	122.45

14	-117.14	58.79	-103.84	72.72	131.27	104.93
15	-116.77	59.28	-104.86	71.91	131.24	99.66
16	122.41	-53.09	105.27	-70.81	130.77	122.45
17	-120.92	54.98	-108.49	67.89	131.16	104.98
18	-120.18	55.73	-110.18	66.22	131.16	99.70

Table S4. Calculated the emission (λ_{emi}) wavelength (in nm), overlap extent (λ_{OC} in %) for vertical singlet (S_1) and triplet (T_1) energies, and oscillator strength (f_{emi}) at PBE0/6-31+G(d) level of theory using toluene.

Molecules	λ_{emi}	λ_{OC}		f_{emi}
		S_1	T_1	
1	420.02	0.20	0.61	0.035
2	469.55	0.51	0.54	0.021
3	483.32	0.50	0.52	0.020
4	511.07	0.13	0.24	0.007
5	581.66	0.13	0.51	0.003
6	605.29	0.15	0.44	0.009
7	471.56	0.05	0.59	0.001
8	539.12	0.05	0.59	0.000
9	558.32	0.05	0.55	0.001
10	415.7	0.19	0.61	0.032
11	462.68	0.55	0.56	0.024
12	476.44	0.51	0.53	0.024
13	483.91	0.15	0.54	0.004
14	541.91	0.18	0.48	0.005
15	556.67	0.19	0.47	0.011
16	486.43	0.05	0.62	0.001
17	554.17	0.09	0.59	0.000
18	552.89	0.09	0.55	0.006

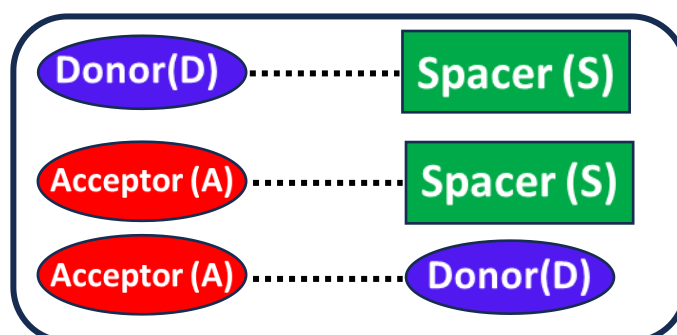


Table S5: Charge transfer analysis based on the S₁ state through interfragment charge transfer (IFCT) among the designed molecular fragments.

Molecules	D-S	A-S	A-D	CT	LE
1	-0.0133	-0.5833	-0.3300	94.21	57.80
2	-0.0025	0.0270	-0.0405	13.159	86.841
3	-0.0015	0.0345	-0.0226	10.055	89.343
4	-0.0368	-0.1982	-0.7309	97.208	2.792
5	-0.0343	-0.1887	-0.7448	97.307	2.693
6	-0.0378	-0.1792	: -0.74182	96.531	3.469
7	-0.0601	-0.0020	-0.9238	98.604	1.396
8	-0.0521	-0.0040	-0.9289	98.52	1.48
9	-0.0477	-0.0050	-0.9317	98.478	1.522
10	-0.0123	-0.5399	-0.3738	94.689	5.311
11	-0.0039	0.0345	-0.0605	15.067	84.933
12	-0.0026	0.0349	-0.0401	12.556	87.444
13	-0.0217	-0.3629	-0.5710	96.611	3.389
14	-0.0282	-0.2146	-0.6630	91.865	8.135
15	-0.0263	-0.1918	-0.6560	88.966	11.034
16	-0.0658	-0.0035	-0.9102	97.98	2.02
17	-0.0554	-0.0122	-0.9107	97.925	2.075
18	-0.0512	-0.0133	-0.9134	97.898	2.102

Additional Computational Details

The intramolecular re-organization energy for the RISC rate is,

$$\lambda_{\text{RISC}} = E_{\text{T}}^{\text{S}} - E_{\text{S}}^{\text{S}} \quad (1)$$

where E_{T}^{S} represent the energy of the singlet state at the triplet state geometry, and E_{S}^{S} represent the energy of the singlet state at the singlet state geometry. In this regard, the intramolecular reorganization energy for RISC is calculated for selected molecules. The overall reorganization energy encompasses both intramolecular reorganization and contributions from the external environment. Therefore, when determining the rates of ISC and RISC, we factored in a total reorganization energy of 0.20 eV. This value encapsulates the effects of relaxations induced by the medium, a topic extensively discussed in previous studies.²

Table S6. Calculated the intramolecular reorganization energies for selected molecules at PBE1PBE/6-31+G(d) level of theory.

Molecules	E_{S1}	E^*_{S1}	Λ (in Hartree)	λ (in eV)
	(S_1 geometry)	(T_1 geometry)	S_1-T_1	S_1-T_1
1	-2443.0578	-2443.0513	0.0065	0.18
4	-2444.2395	-2444.2384	0.0011	0.03
7	-2560.8448	-2560.8397	0.0051	0.14
10	-2459.0847	-2459.0782	0.0065	0.18
11	-3104.8711	-3104.8681	0.0030	0.08
12	-7107.0161	-7107.0103	0.058	0.16

Delayed fluorescence rate, Quantum yields, Internal, and External quantum efficiency³⁻⁵

The delayed fluorescence rate constant can be calculated theoretically by using the equation,

$$K_{TADF}^{-1} = K_r^{-1} + K_{RISC}^{-1} \quad (2)$$

The external quantum efficiency (Φ_{EQE}) can be calculated by,

$$\Phi_{EQE} = \Phi_{IQE} * \eta_{out} \quad (3)$$

The value of the output sheet coupling (η_{out}) typically ranges between 0.2 and 0.3.

The internal quantum efficiency (Φ_{IQE}) can be calculated by,

$$\Phi_{IQE} = \eta_r(S_1) \Phi_r + \eta_r(S_1) \Phi_{ISC} \Phi_{RISC} + \eta_r(T_1) \Phi_{RISC} \quad (4)$$

where $\eta_r(S_1) = 0.25$ and $\eta_r(T_1) = 0.75$ are the branching ratios of the formation of singlet and triplet excitons, respectively. The efficiency of radiative (Φ_r), inter-system crossing (Φ_{ISC}), and reverse-intersystem crossing rate (Φ_{RISC}) can be calculated by,

$$\Phi_r = 1 - \Phi_{ISC} \quad (5)$$

$$\Phi_{ISC} = \frac{K_{ISC}}{K_r} \quad (6)$$

$$\Phi_{\text{RISC}} = \frac{\Phi_{\text{TADF}}}{\Phi_{\text{ISC}}} \quad (7)$$

$$\Phi_{\text{TADF}} = \frac{K_{\text{ISC}} * \Phi_{\text{r}} * K_{\text{RISC}}}{K_{\text{r}} * K_{\text{TADF}}} \quad (8)$$

The photoluminescence quantum yield (PLQY) can be calculated by,

$$\text{PLQY} = \Phi_{\text{r}} + \Phi_{\text{TADF}} \quad (9)$$

Table S7. Calculated the delayed fluorescence rate (K_{TADF} in 10^{+05} s^{-1}), internal quantum efficiency (Φ_{IQE}), external quantum efficiency (Φ_{EQE} %), photoluminescence quantum yield (PLQY %), and (FWHM in nm) for three molecules.

Molecules	K_{TADF}	Φ_{IQE}	Φ_{EQE}	PLQY	FWHM
4	2.75	0.99	24.68	99.77	35
5	2.07	0.60	14.74	77.17	60
6	12.9	-	-	-	48

Table S8. Calculated the Huang-Rhys factors for molecule 1.

Mode	Huang-Rhys factors	Frequency
1	1.71	9.3765
2	6.33	11.4439
3	12.53	15.8225
4	0.12	21.0183
5	0.10	24.9996
6	0.51	32.4219
7	0.13	32.858
10	0.04	51.2839
11	0.17	56.0157
12	0.34	59.5836
14	0.12	74.5586
15	0.01	76.5916
16	0.14	81.6699
17	0.03	94.6635
18	0.49	101.2088
19	0.01	112.5404
20	0.01	126.5712
21	0.31	130.4807
22	0.30	143.2584
23	0.11	149.4476
24	0.02	156.4414
28	0.07	207.2308

29	0.06	214.5698
30	0.35	230.2214
31	0.02	233.1291
33	0.01	243.0192
35	0.06	248.1499
36	0.01	264.2723
41	0.01	290.1434
42	0.05	296.2565
43	0.02	297.9415
44	0.01	299.7628
45	0.07	309.8171
50	0.02	348.6109
52	0.02	362.0539
55	0.05	384.5339
56	0.02	403.0138
58	0.58	423.7637
59	0.30	429.0714
60	0.01	430.0193
63	0.21	445.0311
64	0.02	447.6789
65	0.68	450.5864
66	0.06	454.1103
67	0.02	460.4182
68	0.02	460.894
69	0.02	476.5854
71	0.03	488.517
77	0.01	545.7835
78	0.02	569.831
87	0.01	628.9832
92	0.02	663.4708
93	0.01	669.6923
95	0.04	677.1641
96	0.02	687.0778
100	0.05	742.421
107	0.11	768.0739
111	0.01	782.6454
112	0.01	784.5857
119	0.02	855.0778
160	0.07	1059.417
169	0.01	1128.2013
170	0.01	1137.2777

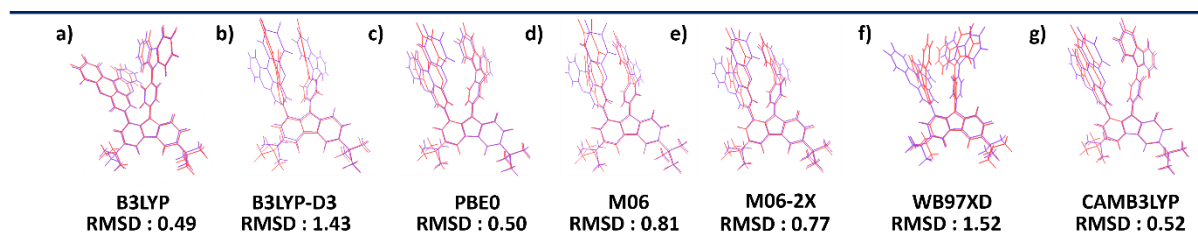


Figure S1. Structural comparison between the crystal structure (violet) and the optimized S_0 state (red) of molecule (1), calculated using various functionals with the 6-31+G(d) basis set.

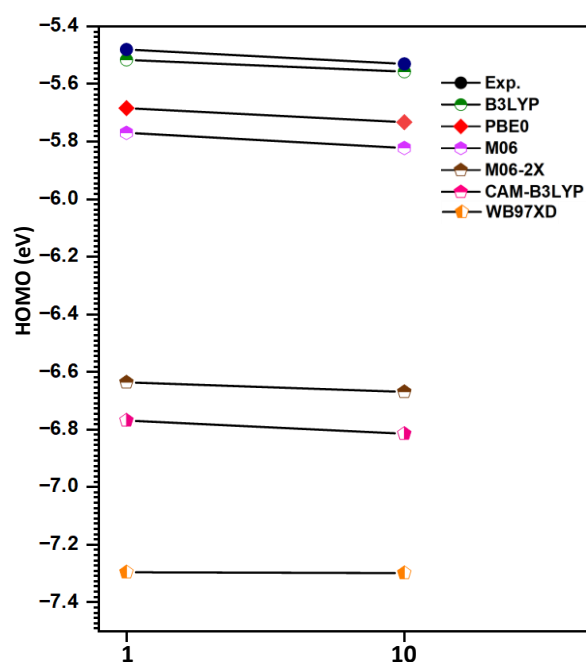


Figure S2. Comparison of HOMO energy for experimental molecules with computed results at different functionals with 6-31+G(d) basis set.

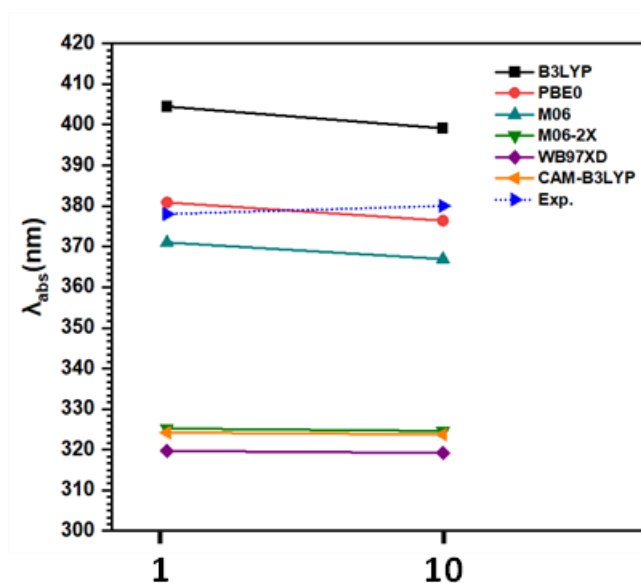


Figure S3. Comparison of absorption wavelength (λ_{abs}) for experimental molecules with computed results at different functionals with 6-31+G(d) basis set.

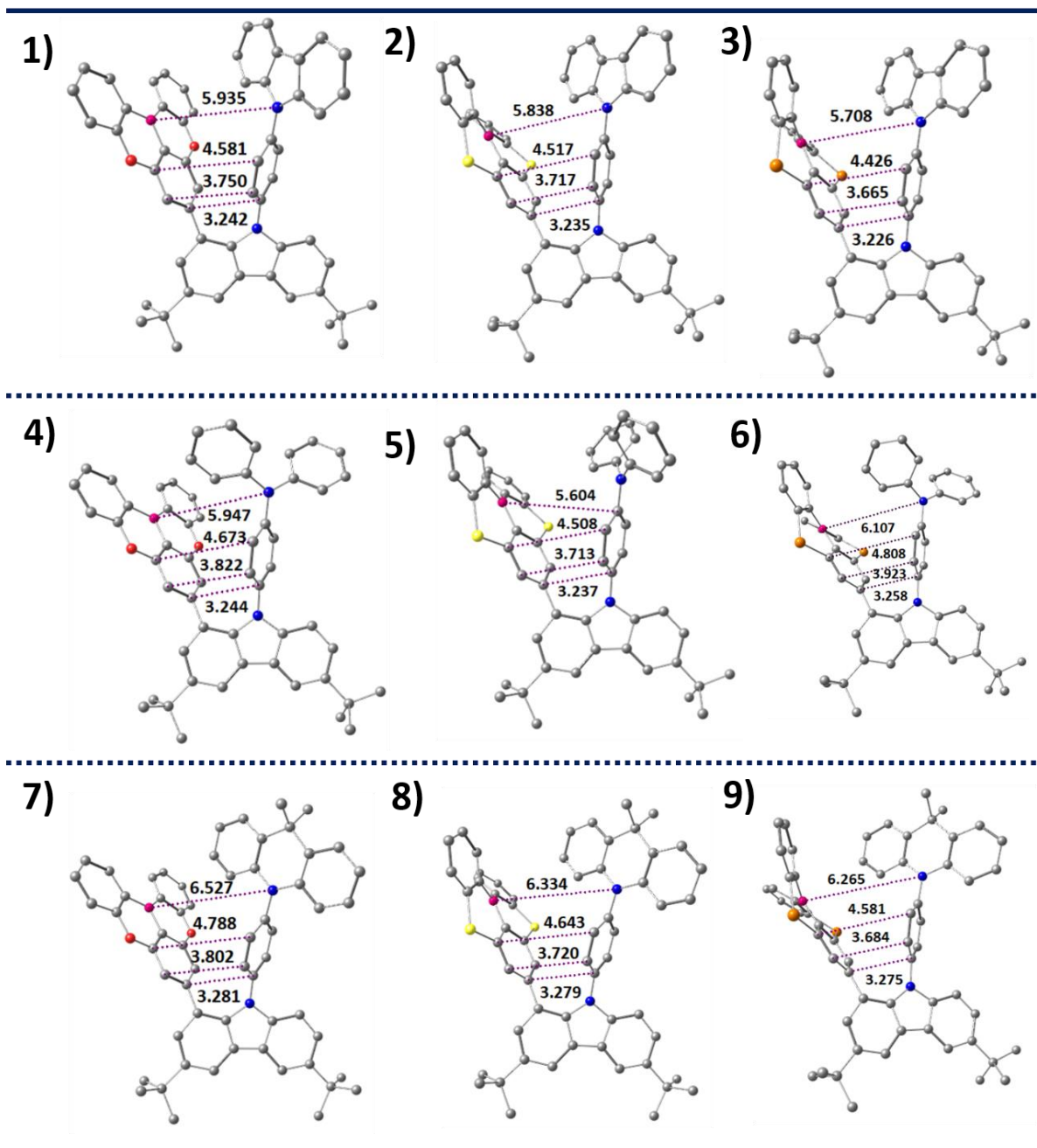


Figure S4. Optimized geometry of designed molecules (1-9) at B3LYP/6-31+G(d) level of theory.

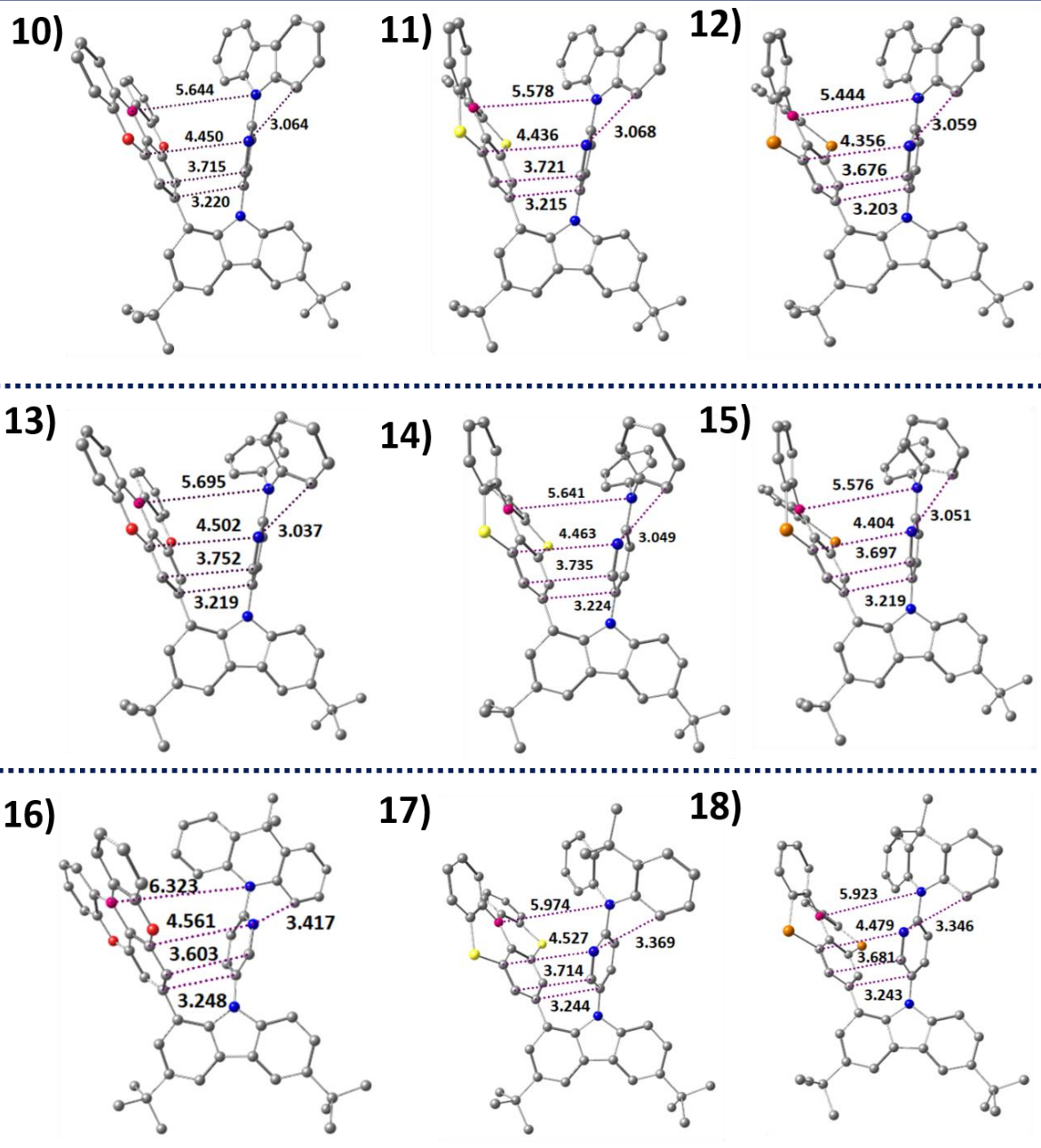


Figure S5. Optimized geometry of designed molecules (10-18) at B3LYP/6-31+G(d) level of theory.

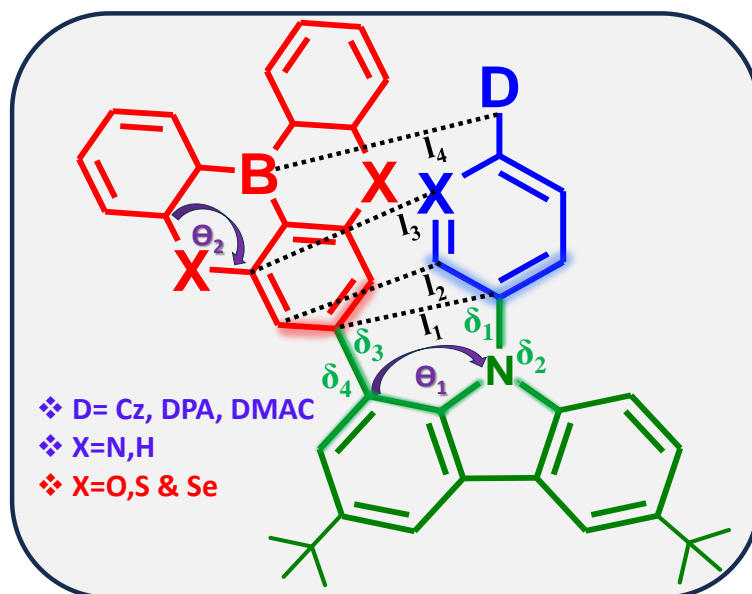


Figure S6. The selected bond length (l), dihedral angles (δ), and bond angle (θ) for designed molecules.

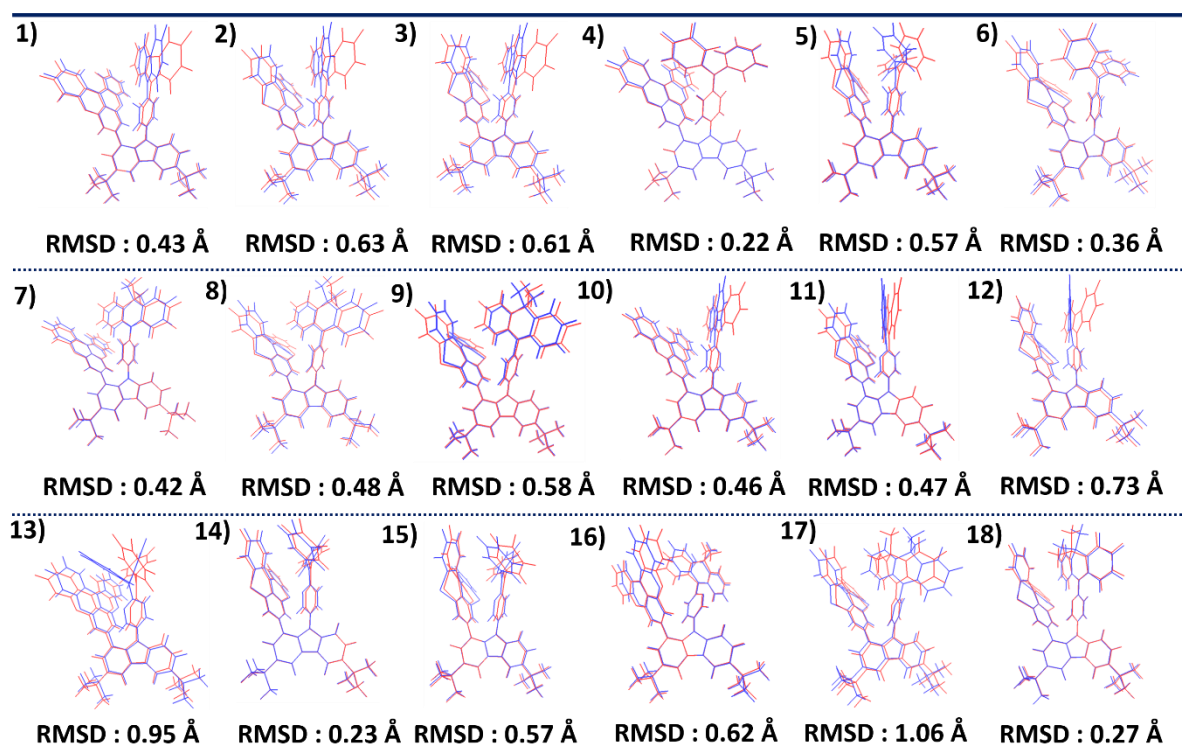


Figure S7. Structural differences between the S_1 and T_1 states for designed molecules (color codes: blue for S_1 and red for T_1).

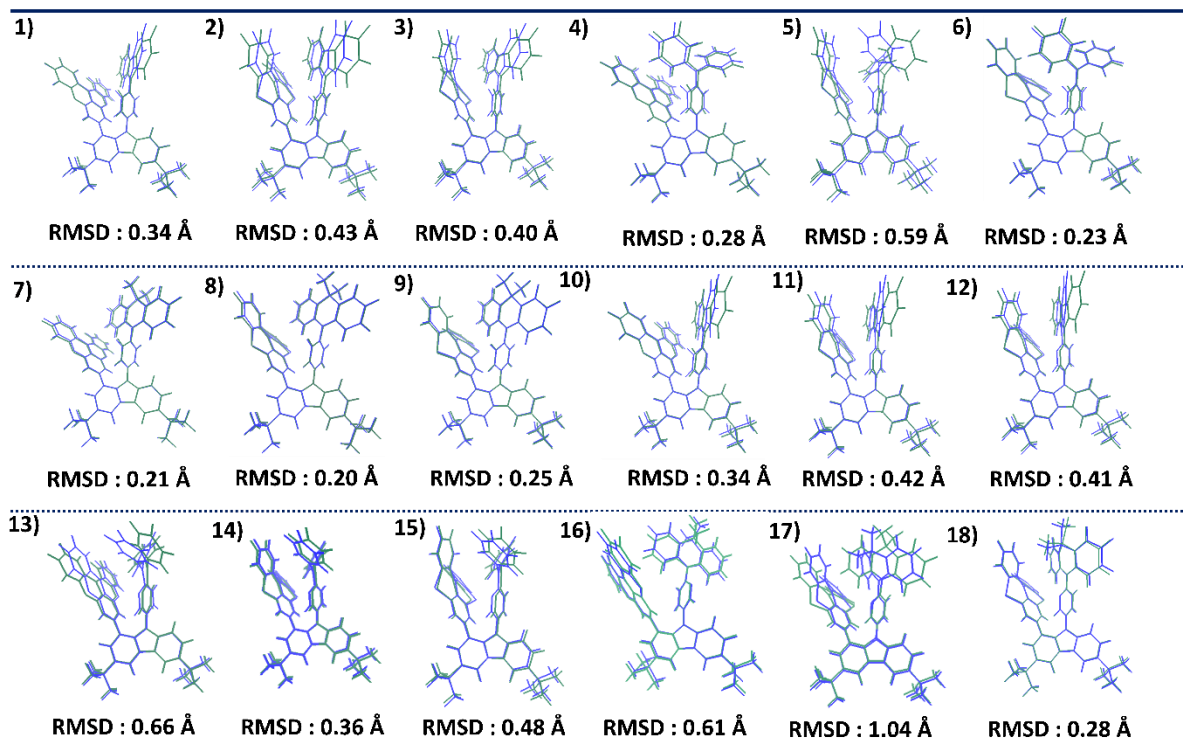


Figure S8. Structural differences between the S_0 and S_1 states for designed molecules (color codes: green for S_0 and blue for S_1).

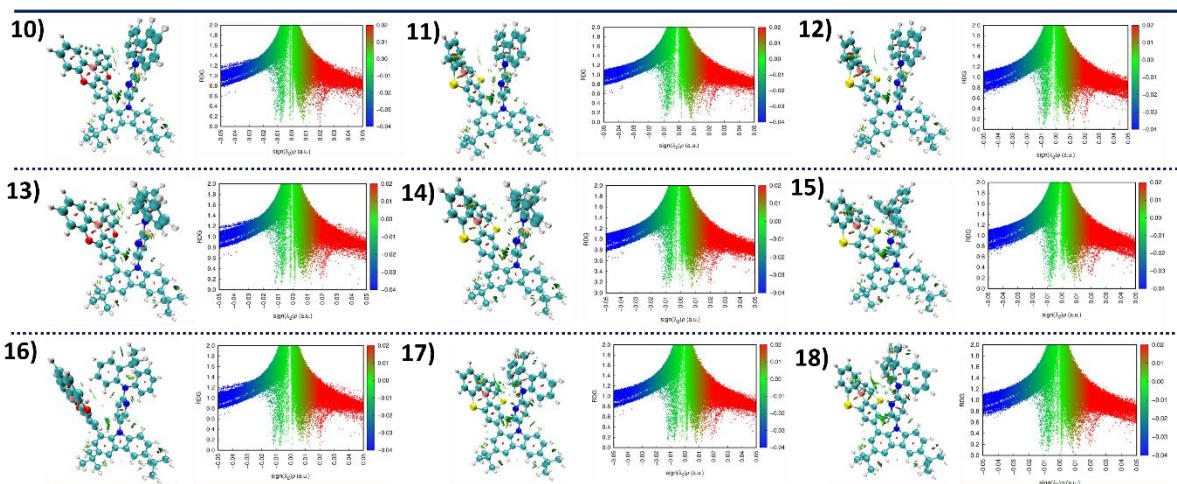


Figure S9. Visualization of non-covalent interactions (NCI) through RDG isosurfaces and scatter plots for (10-18) molecules.

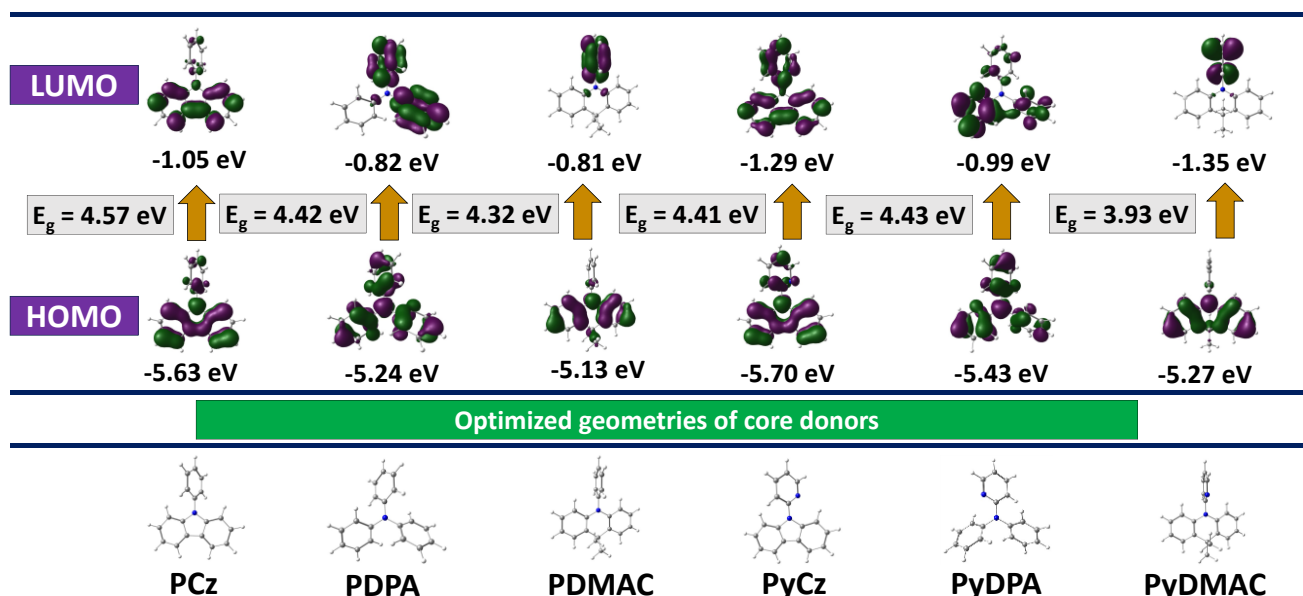


Figure S10. Frontier molecular orbital (FMOs) and optimized geometries of core donors (iso-surface value = 0.02 au) using B3LYP/6-31+G(d) level of theory.

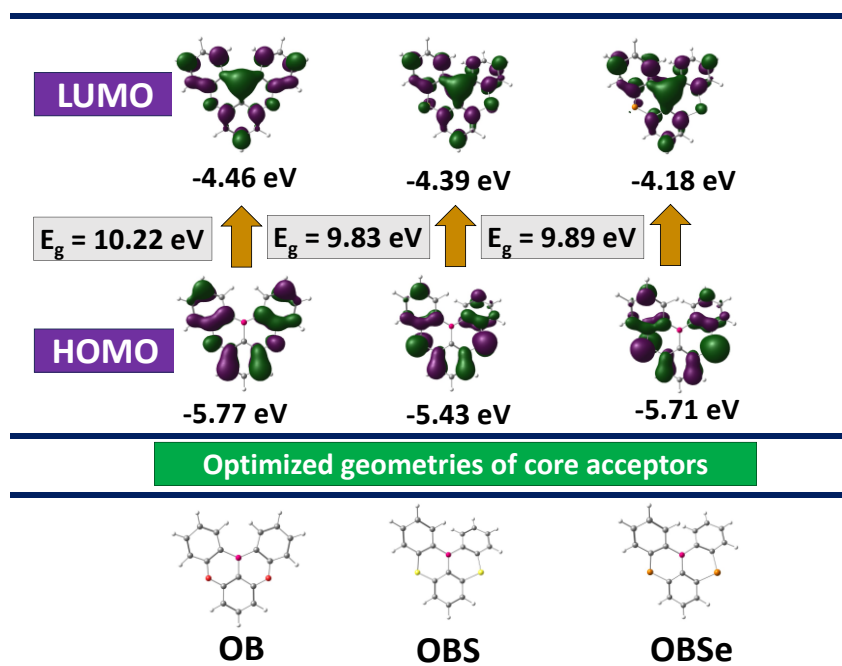


Figure S11. Frontier molecular orbitals (FMOs) and optimized geometries of core acceptors (iso-surface value = 0.02 au) using B3LYP/6-31+G(d) level of theory.

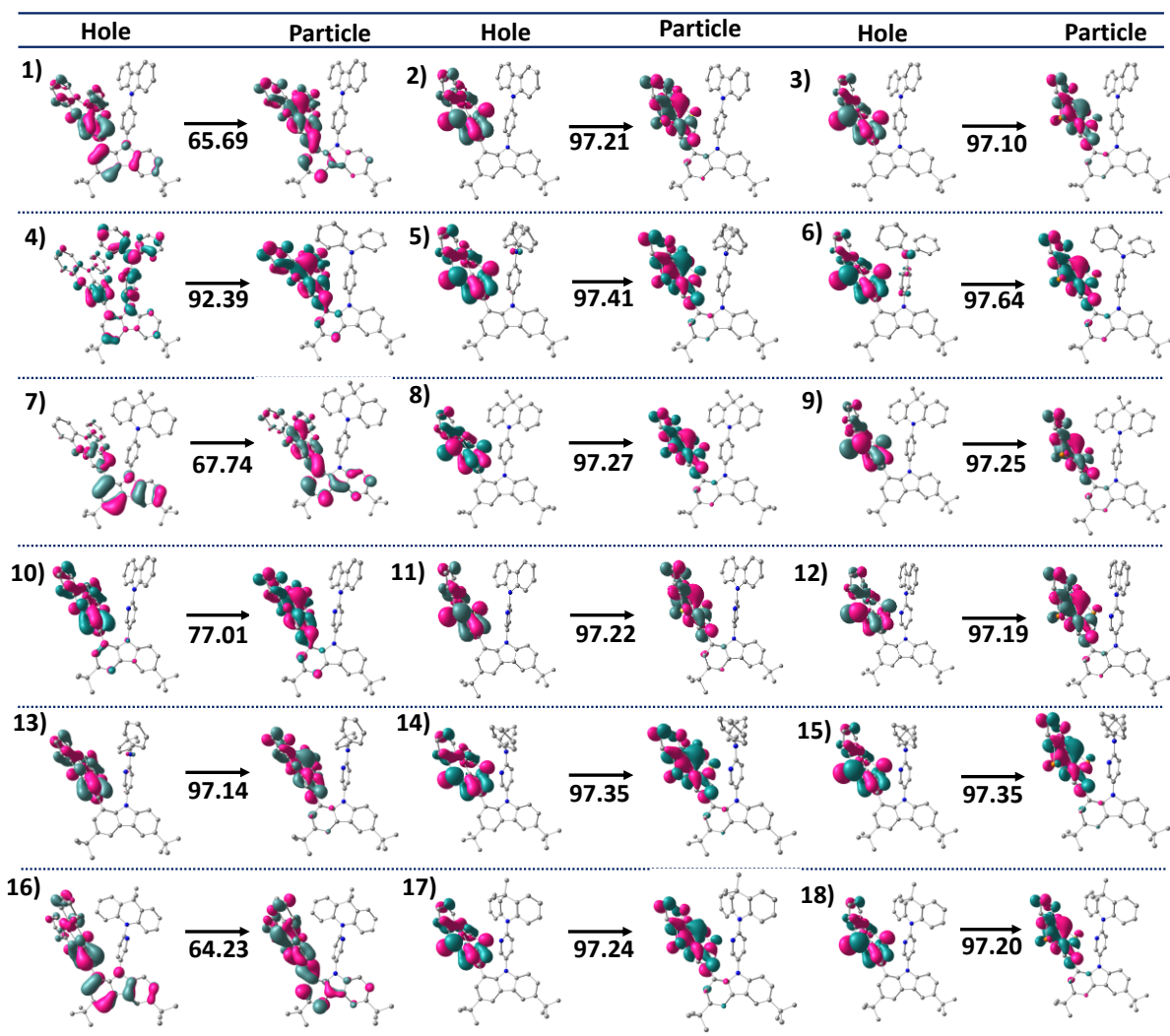


Figure S12. NTOs (iso-surface value = 0.02 a.u.) of designed molecules for T_1 state at PBE0/6-31+G(d) in the toluene medium.

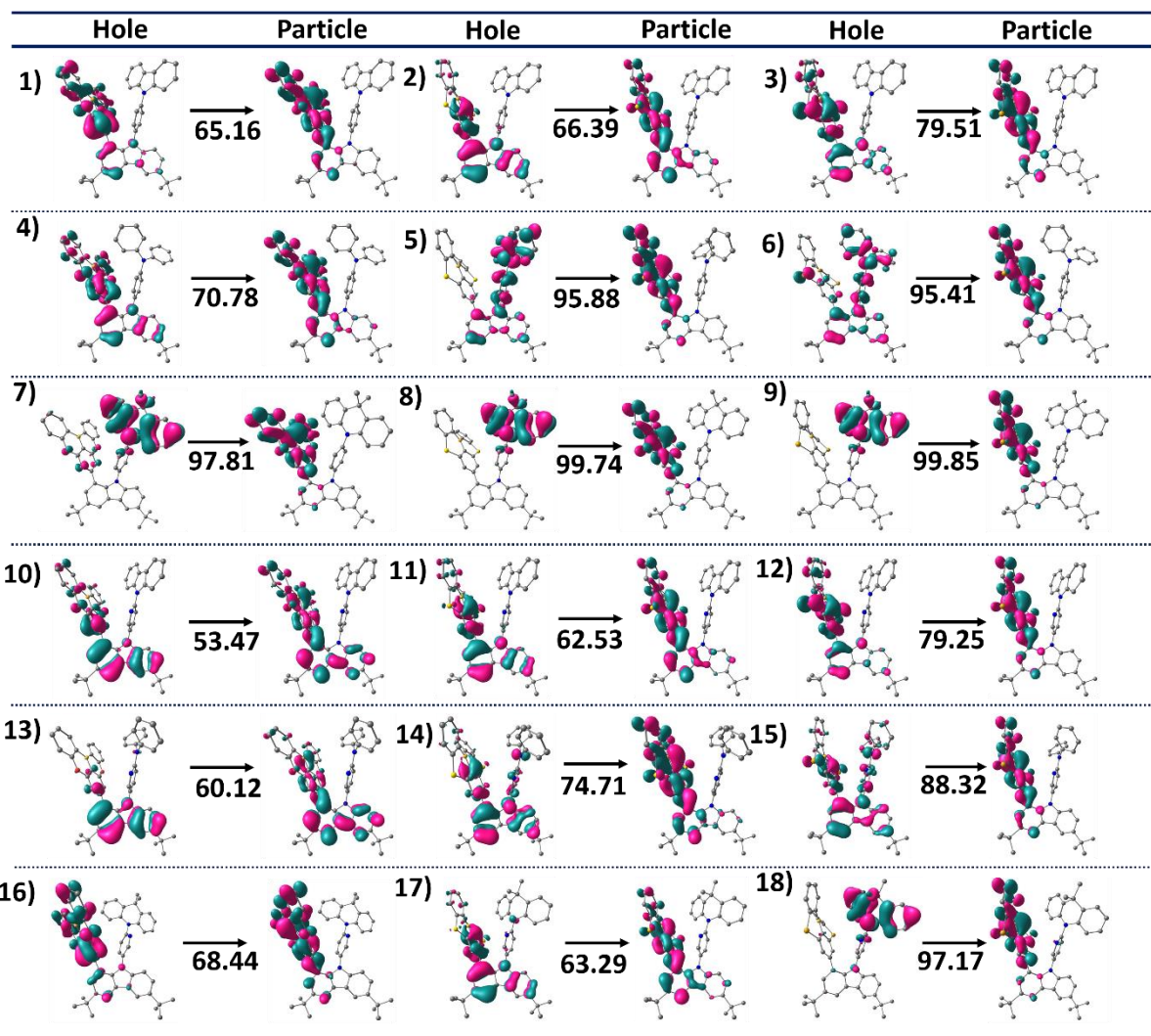


Figure S13. NTOs (iso-surface value = 0.02 a.u.) of designed molecules for T₂ state at PBE0/6-31+G(d) in the toluene medium.

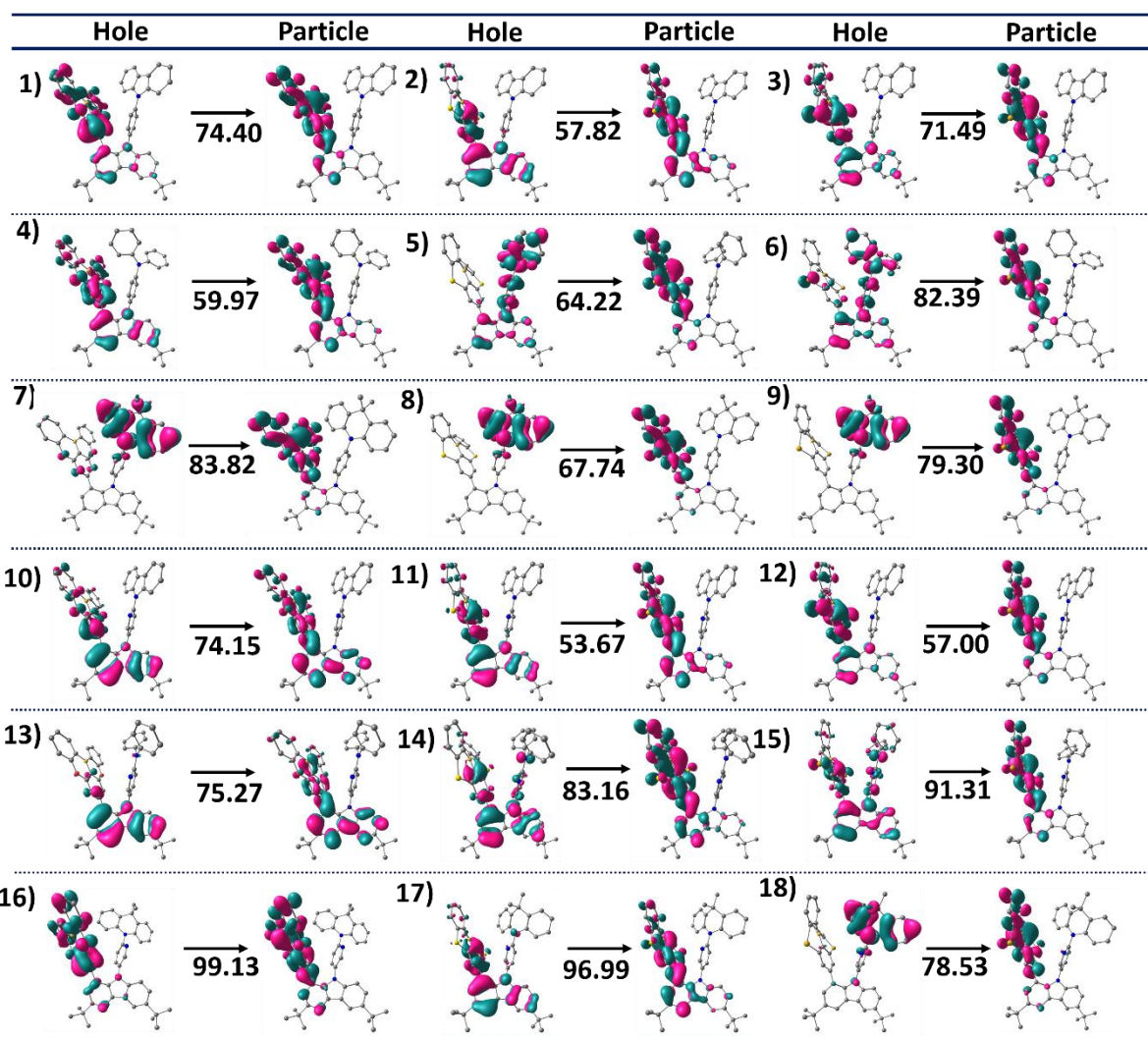


Figure S14. NTOs (iso-surface value = 0.02 a.u.) of designed molecules for T₃ state at PBE0/6-31+G(d) in the toluene medium.

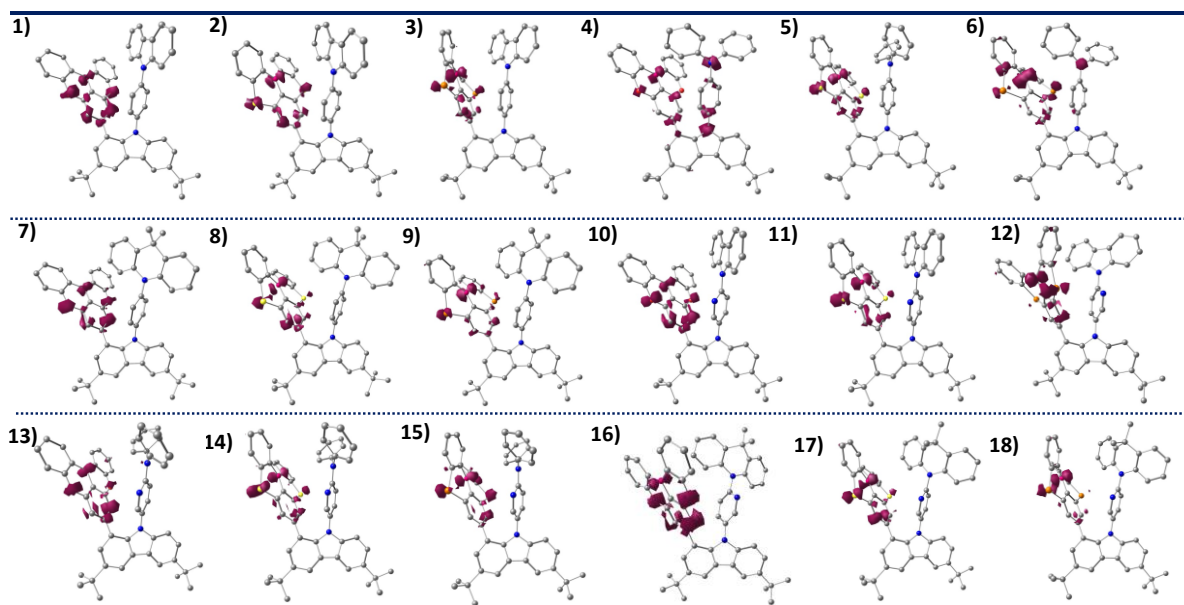


Figure S15. Spin density distributions of the designed molecules in their T_1 state, computed at the PBE0/6-31+G(d) level of theory.

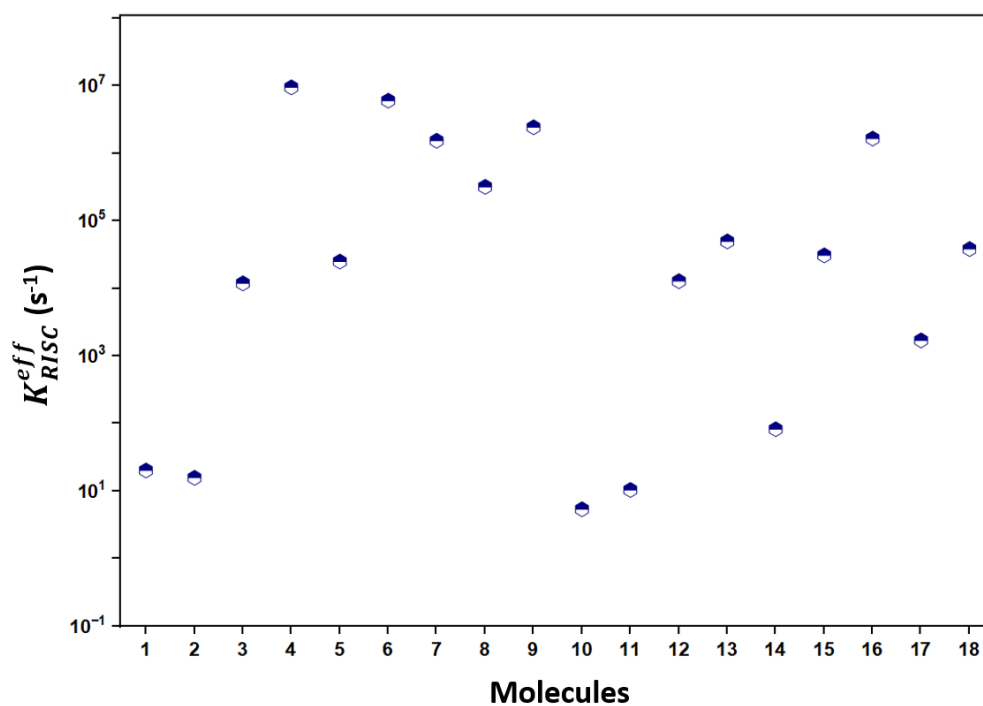


Figure S16. The effective RISC rate (K_{RISC}^{eff}) constant for all designed molecules.

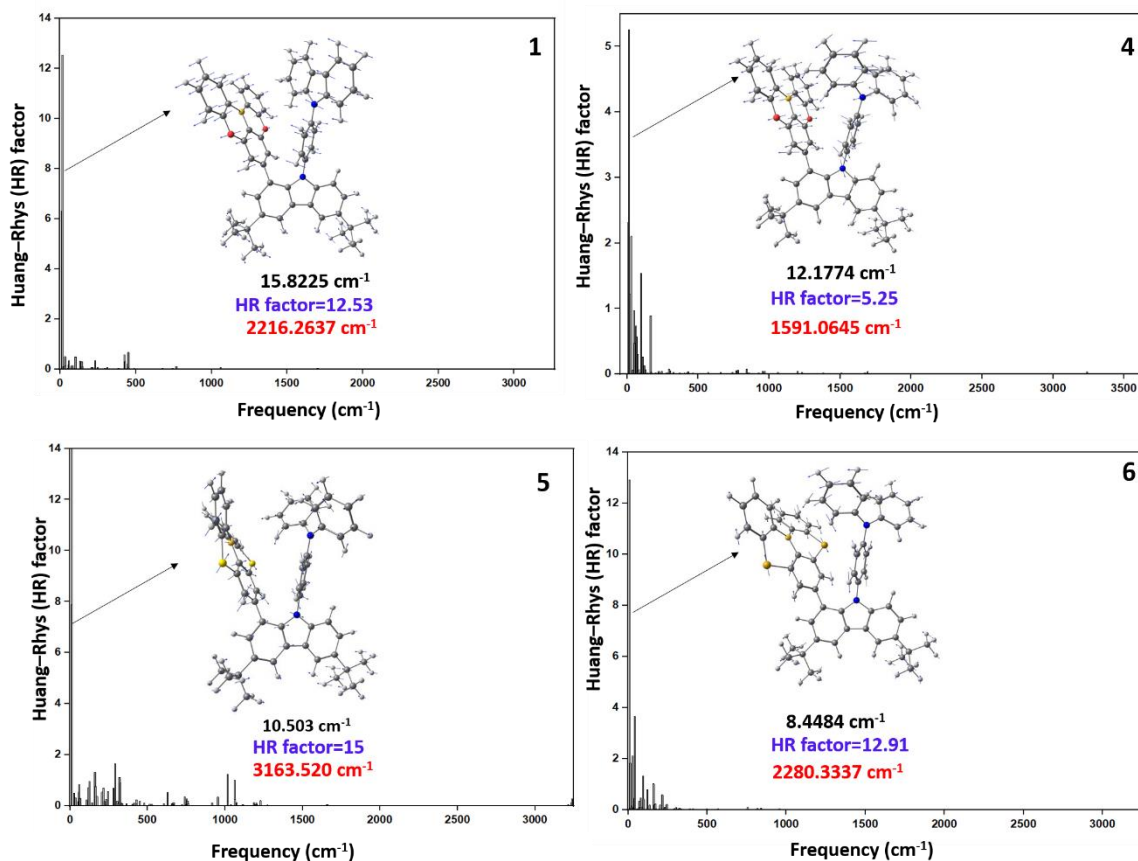


Figure S17. Calculated HR factors of all vibrational modes and reorganization energy (in red colour) in the $S_1 \rightarrow S_0$ transition of molecules 1, 4, 5, & 6.

Reference

- (1) Yang, T.; Qiu, N.; Lan, X.; Dong, X.; Tang, B. Z.; Zhao, Z. *J. Phys. Chem. C.*, 2024, **128** (38), 16085–16092.
- (2) P. K. Samanta, D. Kim, V. Coropceanu and J.-L. Brédas, *J. Am. Chem. Soc.*, 2017, **139**, 4042–4051.
- (3) Endo, A.; Sato, K.; Yoshimura, K.; Kai, T.; Kawada, A.; Miyazaki, H.; Adachi, C. *Appl. Phys. Lett.*, 2011, **98**, 083302.
- (4) Lee, S. Y.; Yasuda, T.; Komiyama, H.; Lee, J.; Adachi, C. *Adv. Mater.*, 2016, **28**, 4019–4024
- (5) Shakeel, U.; Singh, J. *Org. Electron.*, 2018, **59**, 121–124